

GEOMETRIC RELATIVE ORBITAL ELEMENT SET FOR MOTION NEAR A PERIODIC ORBIT WITH OSCILLATORY MODES

Ian Elliott* and Natasha Bosanac†

An important framework for relative trajectory design around periodic multi-body orbits is the description of the relative state between two spacecraft in a non-Keplerian environment. To characterize relative motion around a periodic orbit with oscillatory modes in the circular restricted three-body problem, a set of geometry-based relative elements are defined using first-order quasi-periodic motion expressed in a Hill frame. Mappings between the relative elements and relative Cartesian state elements are derived. The relative elements are used to straightforwardly design transfers for impulsive formation reconfiguration around periodic orbits with oscillatory mode in the Earth-Moon system.

INTRODUCTION

The relative dynamics between two spacecraft in multi-body gravitational environments is emerging as a topic of interest as new mission concepts leveraging formations of spacecraft following periodic orbits and quasi-periodic orbits are explored. To build upon decades of formation flying experience in predominantly two-body environments, framework parallels must be drawn between the development of two-body and three-body relative motion analysis techniques. Since the early study of spacecraft formation flying in circular orbits by Clohessy and Wiltshire¹ and elliptical orbits by Tschauner and Hempel,² local relative dynamics between two spacecraft have been examined using equations of relative motion written using a local-vertical, local-horizontal (LVLH) reference frame. While equations of motion written in an LVLH frame have been studied extensively in two-body environments,³ recently Franzini and Innocenti have explored equations of motion for formations of spacecraft in a restricted three-body system in an LVLH frame defined relative to one of the primary bodies.^{4,5} While the description of relative Cartesian states in an LVLH frame is useful for simulating relative measurements and navigation, the description of relative states via a set of relative orbital elements can provide more geometric insight and aid relative transfer design.

Relative orbital element sets have been widely used as an analysis tool for describing relative motion in two-body environments. Authors including Lovell and Tragesser,⁶ Healy and Henshaw,⁷ and Bennett and Schaub⁸ have used variations of geometric relative orbital element sets to describe solutions to the Clohessy-Wiltshire (CW) equations. In Healy and Henshaw's work, the state of a chaser spacecraft is defined using a relative ellipse centered at the target spacecraft to provide geometric insight into the relative state of the chaser spacecraft in the LVLH frame. Using this approach, parallels are drawn to a classical Keplerian orbital element description of motion in a two-body

*Graduate Research Assistant, Colorado Center for Astrodynamics Research, Smead Aerospace Engineering Sciences, University of Colorado Boulder, Boulder, CO 80303

†Assistant Professor, Colorado Center for Astrodynamics Research, Smead Aerospace Engineering Sciences, University of Colorado Boulder, Boulder, CO 80303

environment. In fact, relative ellipses centered at the International Space Station served as an important geometric structure for Space Shuttle rendezvous and proximity operations.^{9,10} In addition to describing natural motion in two-body environments, differencing classical orbit elements has been studied to develop guidance and control strategies for two-body environments, including recent work by Anderson and Schaub,¹¹ and Roscoe et al.¹² A comprehensive survey of spacecraft relative motion dynamics models was conducted by Sullivan et al. that illustrates the widespread use of different orbital element sets to describe relative motion.³

In the context of three-body gravitational environments, the natural motion in the vicinity of periodic orbits has been studied by several authors.^{13,14} Numerous formulations of formation control strategies in the vicinity of periodic orbits have also been introduced.^{15,16} Notably, mode analysis of a reference periodic orbit was used by Scheeres et al.¹⁷ to develop a stabilizing control law based on the quasi-periodic motion emanating from a periodic orbit in the Hill problem. The use of quasi-periodic motion as a structure for spacecraft formations was explored by Baresi and Scheeres in the context of zonal harmonic dynamics around the Earth using an LVLH frame to visualize quasi-periodic motion relative to a target spacecraft.¹⁸ The Circular Restricted Three-Body Problem (CR3BP) provides an autonomous approximation of the motion in the three-body system expressed using a rotating frame defined by the two primary bodies and contains several dynamical solutions, including periodic and quasi-periodic orbits.¹⁹ To compute quasi-periodic orbits in the CR3BP, Olikara and Scheeres use the eigenvector corresponding to a complex eigenvalue of the periodic orbit's monodromy matrix to define a relative ellipse as an initial guess for computing nonlinear quasi-periodic motion.²⁰

In this paper, a framework for describing relative motion in the CR3BP around a periodic orbit with oscillatory modes via a geometric relative orbital element set is introduced. The six-element set is based on the geometry of first-order quasi-periodic motion relative to a periodic orbit, as defined by the eigenvector corresponding to a complex eigenvalue of the periodic orbit's monodromy matrix. Differing to previous studies, the first-order approximation of quasi-periodic motion is computed within a LVLH frame relative to a target spacecraft traveling on a periodic orbit in the CR3BP. For first-order relative dynamics around the periodic orbit, the element set is demonstrated to have a two-dimensional equilibrium set corresponding to first-order quasi-periodic tori. However, the element set is suitable for providing insight into nonlinear relative motion under the assumptions of the CR3BP for small separations from the periodic orbit. Potential applications of the work presented in this paper include rendezvous and proximity operations around a cislunar near-rectilinear halo orbit (NRHO), in-space assembly at periodic orbits around the Sun-Earth or Earth-Moon equilibrium points, safe trajectory design for proximity operations, and general spacecraft formation establishment and control leveraging quasi-periodic relative motion in three-body environments.

The presented work contains a derivation of relative equations of motion in the CR3BP and a description of the relative element set used to develop examples of formation reconfiguration maneuvers for a chaser spacecraft near a periodic orbit in the CR3BP. The first section examines the natural dynamics of a single spacecraft under the gravitational influence of two primary bodies, including acceleration in an inertial frame and a review of the assumptions, nondimensionalization scheme, and reference frame. The second section introduces the relative motion problem and explores the relative dynamics of two spacecraft under the gravitational influence of two primary bodies. Within this section, a LVLH reference frame local to the target spacecraft is defined. Equations of relative motion are then defined for the chaser spacecraft relative to the target spacecraft observed from the LVLH frame. In the third section, a review of stability analysis and computa-

tion of quasi-periodic motion in the context of periodic orbits in the CR3BP is discussed. A set of geometry-based relative orbital elements are introduced to describe the state of the chaser spacecraft relative to the target, including forward and inverse mappings between elements and relative Cartesian state. An alternative non-singular element set is also introduced to avoid a singularity in the mapping of the geometric element set. Finally, the last section demonstrates applications of the relative orbital element set to impulsive formation reconfiguration within the context of an Earth-Moon (EM) L_2 halo orbit and an EM distant retrograde orbit (DRO). The examples are selected to demonstrate the use of geometric insight from the relative orbital element set to develop constraint formulations and initial guess generation for single-shooting targeting schemes. Additionally, the constraint formulation via relative orbital elements may be applied across various fixed points along a periodic orbit and across various reference periodic orbits for the target spacecraft.

DYNAMICS IN A THREE-BODY ENVIRONMENT

In the restricted three-body problem, a spacecraft is assumed to be influenced by the point mass gravitational effects of two constant-mass primary bodies, P_1 and P_2 , while the gravitational effect of the spacecraft on the two primary bodies is negligible. Under these assumptions, the barycenter of the two primary bodies serves as an inertial observer for the motion of the spacecraft. The position vector of a spacecraft relative to the system's barycenter is defined as \vec{r}_3 . The acceleration of a spacecraft due to gravitational effects of P_1 and P_2 as seen by the the inertial observer, $\ddot{\vec{r}}_3$, is

$$\ddot{\vec{r}}_3 = -\mu_1 \frac{\vec{r}_{13}}{r_{13}^3} - \mu_2 \frac{\vec{r}_{23}}{r_{23}^3} \quad (1)$$

where μ_1 and μ_2 are the gravitational parameters of P_1 and P_2 respectively.²¹ Within this paper, relative vector notation is defined as

$$\vec{r}_{13} = \vec{r}_3 - \vec{r}_1 \quad (2)$$

For practical analysis of spacecraft motion, the acceleration of the spacecraft relative to one of the primary bodies is often of interest. The spacecraft acceleration defined in Eq. 1 can be rearranged to express the inertial acceleration of the spacecraft as seen by P_2 , $\ddot{\vec{r}}_{23}$, as²¹

$$\ddot{\vec{r}}_{23} = -\mu_2 \frac{\vec{r}_{23}}{r_{23}^3} - \mu_1 \left(\frac{\vec{r}_{13}}{r_{13}^3} + \frac{\vec{r}_{21}}{r_{21}^3} \right) \quad (3)$$

This expression is valid for any restricted point mass gravitational environment and is the definition of inertial acceleration for the derivation of equations of motions as observed from non-inertial frames. However, the dynamics of a spacecraft in a three-body environment are often simplified through introducing additional assumptions.

The Circular Restricted Three-Body Problem

The CR3BP models the natural motion of a single spacecraft in a multi-body environment subject to additional constraints. The two primary bodies are defined such that the mass of P_1 , m_1 , is greater than or equal to the mass of P_2 , m_2 . The primary bodies are assumed to travel in circular orbits about their mutual barycenter and the mass of the spacecraft is negligible in comparison. A nondimensionalization scheme is applied to length, time, and mass quantities. Length quantities are nondimensionalized by the distance between the two primary bodies such that $|\vec{r}_2 - \vec{r}_1| = 1$. Time quantities are nondimensionalized such that mean motion of the two primaries about their mutual

barycenter is equal to unity. Lastly, mass quantities are nondimensionalized using the total mass of the system. A system mass ratio, μ , is defined as

$$\mu = \frac{m_2}{m_1 + m_2} \quad (4)$$

such that the nondimensional gravitational parameter of the more massive primary body P_1 is $\mu_1 = 1 - \mu$, and the gravitational parameter of the less massive primary body P_2 is $\mu_2 = \mu$.²² A rotating reference frame, denoted by $R : \{\hat{x}, \hat{y}, \hat{z}\}$, is defined by fixing the first axis unit vector, \hat{x} in the direction of P_2 from the barycenter. The third axis, \hat{z} , is defined in the direction of the angular momentum of the P_1 - P_2 system. Finally, the second axis \hat{y} , completes the right-handed coordinate frame. An inertial reference frame is defined, denoted as $N : \{\hat{X}, \hat{Y}, \hat{Z}\}$. The third axis unit vector of the inertial frame \hat{Z} is aligned with the third axis of the rotating frame \hat{z} , such that the transformation between the inertial and rotating frame is a single-axis counter-clockwise rotation of angle ϕ about axis \hat{Z} . Given the assumption of the circular orbits of the primary bodies and nondimensionalization scheme of the CR3BP, the rate of change of angle ϕ is $\dot{\phi} = \omega = 1$. The angular velocity vector of the rotating frame with respect to the inertial reference frame, $\vec{\omega}_{R/N}$, is

$$\vec{\omega}_{R/N} = \hat{z} \quad (5)$$

and is independent of time when expressed in the rotating frame. An illustration of the inertial frame and the rotating frame defined by P_1 and P_2 is depicted in Figure 1. When expressed in the rotating frame, the positions of the two primary bodies relative to the system barycenter are constant: defined as $\vec{r}_1 = \mu \hat{x}$ and $\vec{r}_2 = (1 - \mu) \hat{x}$.

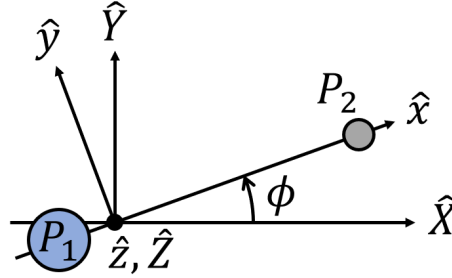


Figure 1. Definition of the inertial and rotating reference frames with the two primary bodies of the CR3BP.

The equations of motion of a spacecraft as observed by the rotating frame provide a useful description of the dynamics of the spacecraft in the CR3BP. The position of a spacecraft relative to the system barycenter, \vec{r}_3 , is expressed in rotating frame components as $\vec{r}_3 = [x, y, z]^T$. Applying the transport theorem twice, the nondimensional acceleration of the spacecraft with respect to the system barycenter as seen by the rotating frame is solved for as

$$\vec{r}_3'' = -(1 - \mu) \frac{\vec{r}_{13}}{r_{13}^3} - \mu \frac{\vec{r}_{23}}{r_{23}^3} - 2 (\vec{\omega}_{R/N} \times \vec{r}_3') - \vec{\omega}_{R/N} \times (\vec{\omega}_{R/N} \times \vec{r}_3) \quad (6)$$

where \vec{r}_3' and \vec{r}_3'' are the velocity and acceleration, respectively, of the spacecraft with respect to the barycenter as seen by and expressed in the rotating frame. Since the positions of the primary bodies with respect to the system barycenter are constant in the rotating frame, these equations of motion are an autonomous dynamical model for approximating natural motion in a three-body environment.

Within the rotating frame, the CR3BP admits several natural dynamical structures, including equilibrium points, periodic orbits, and quasi-periodic orbits. Periodic orbits exhibit periodicity with respect to the rotating frame defined by the two primary bodies. Quasi-periodic motion emanates from periodic orbits with oscillatory modes and trace out the surface of a torus within the rotating frame. For the scope of this work, periodic orbits in the rotating frame are used to define the trajectory of the target spacecraft, assuming the target is governed by the equations of the CR3BP, expressed in the rotating frame. Using equations of relative motion expressed in a Hill frame defined by the target spacecraft in a three-body environment provides a framework for relative motion analysis similar to methods of study in two-body environments.

RELATIVE DYNAMICS IN A THREE-BODY ENVIRONMENT

To describe the relative motion between two spacecraft, two spacecraft are defined: the target spacecraft, denoted by subscript t , and the chaser spacecraft, denoted by subscript c . For the context of this work, the motion of the target spacecraft is governed by the dynamics of the CR3BP and travels on uncontrolled, natural motion. Equations of relative motion are derived for the chaser spacecraft relative to the target spacecraft where both spacecraft are under the gravitational influence of primary bodies P_1 and P_2 . Due to the relevance of periodic orbits in the vicinity of the less massive primary body, e.g. the Moon in the Earth-Moon system, the Hill frame and equations of relative motion are formulated with respect to P_2 . However, the Hill frame and equations of motion are generalizable to analysis with respect to P_1 .

The Hill Frame

A Hill frame, referred to as the LVLH frame for describing dynamics local to the target spacecraft, is defined using the position and velocity of the target spacecraft with respect to the smaller primary, P_2 . The frame is denoted as $O : \{\hat{o}_r, \hat{o}_\theta, \hat{o}_h\}$. The first axis unit vector, \hat{o}_r , is the direction of the target spacecraft as seen by P_2 , defined as

$$\hat{o}_r = \frac{\vec{r}_{2t}}{r_{2t}} \quad (7)$$

This axis direction is also referred to as the ‘‘radial’’ direction. The third unit vector of the Hill frame, \hat{o}_h , is defined in the direction of angular momentum of the target with respect to P_2 , \vec{h}_{2t} . The unit vector is defined as

$$\hat{o}_h = \frac{\vec{h}_{2t}}{h_{2t}} \quad (8)$$

where $\vec{h}_{2t} = \vec{r}_{2t} \times \dot{\vec{r}}_{2t}$ and $\dot{\vec{r}}_{2t}$ is the inertial velocity of the target spacecraft relative to P_2 . This axis is referred to as the ‘‘cross-track’’ direction. The second unit vector, \hat{o}_θ , denoted as the ‘‘along-track’’ direction, completes the right handed coordinate system, and is calculated as²³

$$\hat{o}_\theta = \hat{o}_h \times \hat{o}_r \quad (9)$$

An illustration of the inertial frame and Hill frame described by the target with respect to P_2 is included in Figure 2. The angular velocity of the Hill frame with respect to the inertial frame, $\vec{\omega}_{O/N}$ is influenced by the gravitational effects of both P_1 and P_2 , and is expressed as²³

$$\vec{\omega}_{O/N} = \frac{\vec{h}_{2t}}{r_{2t}^2} + \frac{\vec{r}_{2t}}{h_{2t}} (\ddot{\vec{r}}_{2t} \cdot \hat{o}_h) \quad (10)$$

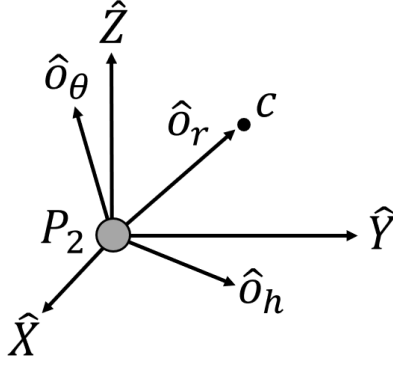


Figure 2. Definition of the inertial and Hill reference frames with the less massive primary body, P_2 , and target spacecraft.

Generally, the time rate of change of $\vec{\omega}_{O/N}$ is nonzero, and is expressed as

$$\dot{\vec{\omega}}_{O/N} = \frac{\dot{h}_{2t}}{r_{2t}^2} - 2 \frac{(\vec{r}_{2t} \cdot \dot{\vec{r}}_{2t}) \vec{h}_{2t}}{r_{2t}^4} + \left(\frac{\dot{r}_{2t}}{h_{2t}} - \frac{r_{2t}(\dot{h}_{2t} \cdot \dot{h}_{2t})}{h_{2t}^3} \right) (\vec{r}_{2t} \cdot \hat{o}_h) + \frac{r_{2t}}{h_{2t}} \left(\ddot{\vec{r}}_{2t} \cdot \hat{o}_h + \dot{\vec{r}}_{2t} \cdot \dot{\hat{o}}_h \right) \quad (11)$$

This expression requires the third time derivative of the target spacecraft's position with respect to P_2 , $\ddot{\vec{r}}_{2t}$, which is computed as

$$\ddot{\vec{r}}_{2t} = -\mu \left(\frac{\dot{\vec{r}}_{2t}}{r_{2t}^3} - 3 \frac{r_{2t}(\vec{r}_{2t} \cdot \dot{\vec{r}}_{2t})}{r_{2t}^5} \right) - (1-\mu) \left(\frac{\dot{\vec{r}}_{1t}}{r_{1t}^3} - 3 \frac{r_{1t}(\vec{r}_{1t} \cdot \dot{\vec{r}}_{1t})}{r_{1t}^5} + \frac{\dot{r}_{21}}{r_{21}^3} - 3 \frac{r_{21}(\vec{r}_{21} \cdot \dot{\vec{r}}_{21})}{r_{21}^5} \right) \quad (12)$$

In addition, the rate of change of the angular momentum unit vector, $\dot{\hat{o}}_h$, is

$$\dot{\hat{o}}_h = \vec{\omega}_{O/N} \times \hat{o}_h \quad (13)$$

With a reference frame established, equations of relative motion that enable a relative state to be straightforwardly propagated in the Hill frame is investigated.

Equations of Relative Motion in a Three-Body Environment

The relative motion of the chaser spacecraft as seen by the target spacecraft is derived in the Hill frame defined by the target spacecraft relative to P_2 . The relative position vector of the chaser spacecraft with respect to the target spacecraft, $\vec{\rho}$, is defined as

$$\vec{\rho} = \vec{r}_c - \vec{r}_t \quad (14)$$

Using the transport theorem and solving for the Hill frame acceleration of $\vec{\rho}$, the equations of relative motion of the chaser are

$$\vec{\rho}'' = \ddot{\vec{\rho}} - \dot{\vec{\omega}}_{O/N} \times \vec{\rho} - 2(\vec{\omega}_{O/N} \times \vec{\rho}') - \vec{\omega}_{O/N} \times (\vec{\omega}_{O/N} \times \vec{\rho}) \quad (15)$$

Note that $\vec{\rho}'$ and $\vec{\rho}''$ denote the velocity and acceleration respectively of $\vec{\rho}$ as seen by the target spacecraft in the Hill frame. The inertial relative acceleration, $\ddot{\vec{\rho}}$, is calculated by differencing the inertial

accelerations of the target and chaser as described by Eq. 3, and is expressed in nondimensional quantities as

$$\ddot{\vec{\rho}} = -\mu \left(\frac{\vec{r}_{2c}}{r_{2c}^3} - \frac{\vec{r}_{2t}}{r_{2t}^3} \right) - (1 - \mu) \left(\frac{\vec{r}_{1c}}{r_{1c}^3} - \frac{\vec{r}_{1t}}{r_{1t}^3} \right) \quad (16)$$

A six-element state of the chaser spacecraft, \vec{q} , relative to the target spacecraft is defined as

$$\vec{q} = \begin{bmatrix} \vec{\rho} \\ \dot{\vec{\rho}} \end{bmatrix} \quad (17)$$

The rate of change of the relative state vector as seen by the target spacecraft in the Hill frame, \vec{q}' , is a function of both the target state and chaser state. Since the relative dynamics of the chaser spacecraft is coupled with the state of the target spacecraft, propagation of the nonlinear equation of relative motion is implemented by numerically integrating the state of the target and chaser spacecraft simultaneously. For a general formation in the Earth-Moon system, time is introduced into the relative dynamics through the position of the Earth relative to the Moon, \vec{r}_{21} . When the assumptions of the CR3BP are applied, this relative position vector simplifies to $\vec{r}_{21} = -\hat{x}$. If the target spacecraft's state is expressed in rotating frame components, time does not explicitly appear in the equations of relative motion. As a result, when the target spacecraft state's dynamics modeled using the CR3BP, integration of the target and chaser spacecraft is performed using a system of 12 scalar and autonomous differential equations.

Quasi-Periodic Relative Motion

For the scope of this paper, the target spacecraft is assumed to follow a periodic orbit with oscillatory modes under the dynamics of the CR3BP. In dynamical systems theory, the stability of a periodic orbit is computed by numerically integrating the state transition matrix, $[\Phi]$, of the periodic orbit for one period of the orbit, T , using the differential equation

$$[\dot{\Phi}] = [A][\Phi] \quad (18)$$

where $[A]$ is the Jacobian of the equations of relative motion evaluated at the target's state at the origin of the LVLH frame, defined as

$$[A] = \left. \frac{\partial \vec{q}'}{\partial \vec{q}} \right|_{\vec{q}_t = \vec{0}} \quad (19)$$

The state transition matrix over one period, $[\Phi(t_0, t_0 + T)]$, is denoted as the monodromy matrix, $[M]$. The eigenvalues of the monodromy matrix reflect the stability characteristics of the periodic orbit.²² Quasi-periodic motion is identified using the eigenvector, \tilde{q} , corresponding to the complex eigenvalue of the monodromy matrix lying on the unit circle. First-order quasi-periodic motion relative to the target spacecraft can be expressed in the LVLH frame as an ellipse centered at the target defined by the real and imaginary components of the eigenvector as the conjugate diameters of the ellipse. The eigenvector is numerically propagated along the periodic orbit using the Jacobian evaluated at the target spacecraft's state at the origin of the LVLH frame. The rate of change of the eigenvector as seen by an observer in the Hill frame \vec{q}' is

$$\vec{q}' = [A]\tilde{q} \quad (20)$$

Once the eigenvector has been computed at the desired time, the relative state of the quasi-periodic reference motion, \tilde{q}^* , is defined as²⁰

$$\tilde{q}^* = \epsilon (\text{Re}(\tilde{q}) \cos \theta + \text{Im}(\tilde{q}) \sin \theta) \quad (21)$$

where ϵ is a small value. Over one revolution of the periodic orbit for a given value of ϵ , the resulting relative ellipse rotates, expands, contracts, and varies in eccentricity in the LVLH frame.

Complex Eigenvector

The relative orbital element set introduced in this paper is coupled with the oscillatory mode of the periodic orbit of the target spacecraft. The eigenvector, \tilde{q} , corresponding to the complex eigenvalue of the monodromy matrix is expressed as a summation of the real and imaginary 6×1 vector components of the eigenvector, \tilde{q}_r and \tilde{q}_i respectively, as

$$\tilde{q} = \tilde{q}_r \pm i \tilde{q}_i \quad (22)$$

The vector of real components of the eigenvector are then separated into two 3×1 vectors corresponding to position and velocity, \vec{r}_r and \vec{v}_r , as

$$\tilde{q}_r = \begin{bmatrix} \vec{r}_r \\ \vec{v}_r \end{bmatrix} \quad (23)$$

Similarly, the vector of imaginary components is separated into two vectors corresponding to position and velocity, \vec{r}_i and \vec{v}_i , as

$$\tilde{q}_i = \begin{bmatrix} \vec{r}_i \\ \vec{v}_i \end{bmatrix} \quad (24)$$

A plane is defined, referred to as the center plane, that is spanned by the real and imaginary position vectors of the eigenvector, \vec{r}_r and \vec{r}_i . A vector normal to the plane, denoted \vec{n} , is defined as

$$\vec{n} = \vec{r}_r \times \vec{r}_i \quad (25)$$

This plane serves as a geometric structure containing ellipses of first-order quasi-periodic relative motion emanating from the target spacecraft's periodic orbit. Since the center plane definition and relative orbital element set are dependent on the complex eigenvector, a scheme to normalize the eigenvector is required for consistent implementation.

The complex eigenvector, \tilde{q} , can be scaled by any complex number $c \in \mathbb{C}$. The eigenvector may also be computed for the monodromy matrix at any point along the periodic orbit. The first step for normalization of the complex eigenvector is to solve for the eigenvalues and eigenvectors of the monodromy matrix via numerical eigendecomposition. If a complex eigenvalue exists, a pair of complex conjugates are returned with complex conjugate eigenvectors corresponding to these eigenvalues. A complex eigenvector as returned from the eigenvector solver is selected, denoted as \tilde{q}_0 . The real and imaginary vector components of the eigenvector, \tilde{q}_r and \tilde{q}_i , are a conjugate diameter definition of an ellipse corresponding to quasi-periodic relative motion in six-dimensional state space. The principal axes of the ellipse defined by the eigenvector provide suitable geometric insight to exploit for normalization of the eigenvector. To compute the principal axes, a singular value decomposition (SVD) is applied to matrix $[E]$, defined as a 6×2 matrix containing the real and imaginary components of the complex eigenvector as returned by the eigenvector solver

$$[E] = [\text{Re}(\tilde{q}_0) \quad \text{Im}(\tilde{q}_0)] \quad (26)$$

The SVD of matrix $[E]$ is written as

$$[E]_{6 \times 2} = [U]_{6 \times 6} [\Sigma]_{6 \times 2} [V]_{2 \times 2}^T \quad (27)$$

The first two columns of matrix $[U]$ are the orthonormal basis vectors for the principal axes of the hyper-ellipsoid: the semi-major axis \vec{a} and semi-minor axis \vec{b} . The diagonal elements of the top two rows of $[\Sigma]$ are the magnitudes of the semi-major and semi-minor axis. The matrix $[V]$ is a rotation matrix, which may be expressed as

$$[V] = \begin{bmatrix} \cos \Theta & \sin \Theta \\ -\sin \Theta & \cos \Theta \end{bmatrix} \quad (28)$$

Extracting Θ , Euler's formula is used to compute the corresponding complex number c as

$$c = e^{\Theta i} = \cos \Theta + i \sin \Theta \quad (29)$$

By scaling the eigenvector returned by the eigendecomposition solver, \tilde{q}_0 , by c , the real components of the eigenvector are aligned with the semi-major axis and the imaginary components are aligned with the semi-minor axis of the ellipse. The eigenvector scaled by c , denoted as \tilde{q}_1 , is written as

$$\tilde{q}_1 = c \tilde{q}_0 \quad (30)$$

This eigenvector is normalized such that the semi-major axis is equal to unity. The normalized eigenvector, denoted \tilde{q}_2 , is computed by dividing \tilde{q}_1 by the magnitude of \vec{r}_r as

$$\tilde{q}_2 = \frac{\tilde{q}_1}{r_r} \quad (31)$$

Finally, two sign checks are applied. The normal unit vector of the plane defined by the real and imaginary position components of \tilde{q}_2 , \hat{n} , expressed in the Hill frame is computed. If $\hat{n}^T \hat{o}_h < 0$, use the complex conjugate of \tilde{q}_2 . If $\vec{a}^T \hat{o}_\theta < 0$, multiply \tilde{q}_2 by -1. The resulting eigenvector, denoted \tilde{q} without a subscript, possess a unique description for use in computations related to the relative element set. An illustration of the normalization process is included in Figure 3.

RELATIVE ORBITAL ELEMENT SET

A set of relative elements is introduced to supply geometric insight into the relative state of the chaser spacecraft from the target spacecraft in the context of quasi-periodic relative motion. The first scalar element, h , describes the distance of the chaser spacecraft from the center plane and possesses units of position. A value of $h = 0$ indicates the chaser spacecraft is on the center plane of the target spacecraft as defined by \hat{n} . The sign of h indicates whether the position of the spacecraft is in the parallel or anti-parallel direction of \hat{n} . The element h is considered as the out-of-plane element, whereas the other elements are the in-plane elements, and correspond to the projection of the position vector of the chaser spacecraft onto the center plane. The second element, ϵ , indicates the size of the relative ellipse that passes through the position of the chaser spacecraft projected on to the center plane and has units of position. When the eigenvector normalization scheme outlined earlier is applied, ϵ corresponds to the semi-major axis in position space of the relative ellipse at the fixed point of the periodic orbit where the monodromy matrix is computed. Since the size of quasi-periodic orbit relative to the periodic orbit changes along the orbit, ϵ only corresponds to the semi-major axis at a single point along the orbit. The third element, θ , is an indication of the

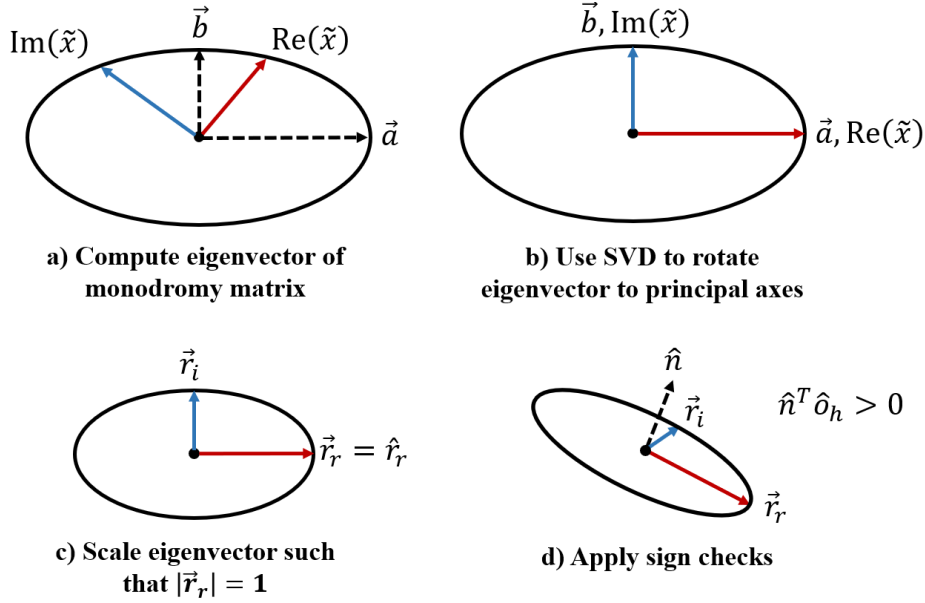


Figure 3. Process for the normalization of the complex eigenvector.

rotation of the chaser from \vec{r}_r around the relative ellipse defined by ϵ , and has units of radians. The three-element set \vec{e} , is summarized as

$$\vec{e} = \begin{bmatrix} h \\ \epsilon \\ \theta \end{bmatrix} \quad (32)$$

The time rate of change of the three scalar relative orbital elements is expressed as a matrix of scalar quantities, $\dot{\vec{e}}$, as

$$\dot{\vec{e}} = \begin{bmatrix} \dot{h} \\ \dot{\epsilon} \\ \dot{\theta} \end{bmatrix} \quad (33)$$

The relative elements supply geometric insight into the state of the chaser spacecraft as a function of nearby first-order quasi-periodic motion relative to the periodic orbit of the target spacecraft. A state on a quasi-periodic torus is approximated by selecting an element set of $h = 0$ with ϵ and θ as free parameters corresponding to the size of the torus and rotation of the chaser spacecraft along the transverse direction of the torus respectively. Under dynamics linearized about the target, first-order quasi-periodic motion exists as an equilibrium set, defined as the set of elements where $h = \dot{h} = \dot{\epsilon} = \dot{\theta} = 0$. In this case, ϵ and θ are constant over time for linearized dynamics, and can provide near-constant values for full nonlinear dynamics near the periodic orbit. A visual of the relative orbital elements is included in Figure 4. The axis of the Hill frame are included with the origin on the target spacecraft to depict the LVLH coordinate system. The real position components of the eigenvector are depicted in red and imaginary components are depicted in blue. The center plane as defined by the eigenvector at the current time is represented in gray. The relative position vector of the chaser spacecraft, $\vec{\rho}$, is also visualized. The relative ellipse defined by ϵ is also illustrated with a representation of the angle θ . Finally, h is included to represent the distance of the chaser from the center plane along the \hat{n} direction. With the definition of the relative elements,

nonlinear mappings are introduced to convert state representations between relative Cartesian states and relative elements.

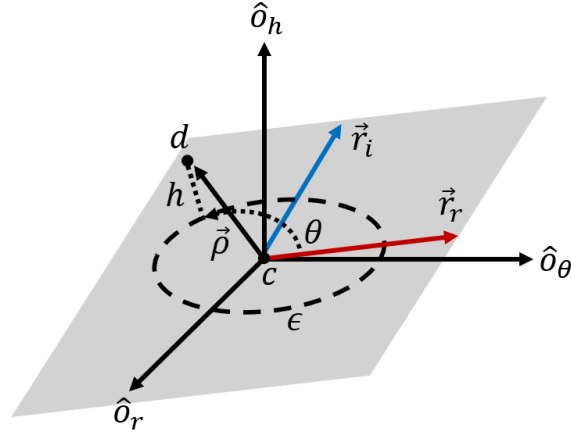


Figure 4. Illustration describing the relative elements h , ϵ , and θ with respect to relative position, $\vec{\rho}$ expressed in the LVLH frame.

Mappings Between Relative Cartesian States and Relative Elements

Together, the relative elements, \vec{e} , and their rate of changes, $\dot{\vec{e}}$, provide a unique description of the state of the chaser relative to the target spacecraft, with the exception of a singularity at $\epsilon = 0$. The Cartesian position of the chaser spacecraft in the Hill frame is expressed as a function of the relative orbital element set as

$$\vec{\rho} = h\hat{n} + \epsilon(\vec{r}_r \cos \theta + \vec{r}_i \sin \theta) \quad (34)$$

This mapping from elements to position is derived from first-order quasi-periodic relative motion defined in Eq. 21, with an additional component corresponding to the out-of-plane components of $\vec{\rho}$ from the center plane. A non-unique mapping occurs when $\epsilon = 0$ and θ becomes undefined. To compute the relative elements given the relative position, $\vec{\rho}$, a set of non-singular quantities, denoted \vec{z} , are first defined as

$$\vec{z} = \begin{bmatrix} h \\ \alpha \\ \beta \end{bmatrix} \quad (35)$$

where α is

$$\alpha = \epsilon \cos \theta \quad (36)$$

and β is

$$\beta = \epsilon \sin \theta \quad (37)$$

The time rate of change of scalar elements of the non-singular quantities, $\dot{\vec{z}}$, is

$$\dot{\vec{z}} = \begin{bmatrix} \dot{h} \\ \dot{\alpha} \\ \dot{\beta} \end{bmatrix} \quad (38)$$

where $\dot{\alpha}$ is

$$\dot{\alpha} = \dot{\epsilon} \cos \theta - \epsilon \dot{\theta} \sin \theta \quad (39)$$

and $\dot{\beta}$ is

$$\dot{\beta} = \dot{\epsilon} \sin \theta + \epsilon \dot{\theta} \cos \theta \quad (40)$$

A matrix, $[R]$ is defined to span the three-dimensional position space and decouples in-plane and out-of-plane bases as

$$[R] = [\hat{n} \quad \vec{r}_r \quad \vec{r}_i] \quad (41)$$

A Cartesian relative position vector is then expressed as a function of $[R]$ and \vec{z} as

$$\vec{\rho} = [R]\vec{z} \quad (42)$$

Then, the non-singular quantities, \vec{z} , are solved for by inverting $[R]$ as

$$\vec{z} = [R]^{-1}\vec{\rho} \quad (43)$$

The matrix $[R]$ is full rank and invertible so long as \vec{r}_r and \vec{r}_i are not collinear. Once \vec{z} has been computed, the in-plane elements are extracted straightforwardly. The element ϵ is computed as

$$\epsilon = \sqrt{\alpha^2 + \beta^2} \quad (44)$$

and the angle θ is computed as

$$\theta = \tan^{-1} \left(\frac{\beta}{\alpha} \right) \quad (45)$$

This nonlinear mapping to the relative orbital elements is a function of both the Cartesian relative position, $\vec{\rho}$, and the eigenvector, \hat{q} , at the current time.

While the mapping between Cartesian relative position and relative orbital elements is independent of velocity, mappings between Cartesian relative velocity and element rate of changes are dependent on the current relative position. By taking the time derivative of Eq. 34, the Cartesian velocity vector as seen by the target spacecraft in Hill frame can be expressed as a function of the elements and the rate-of-change of the elements as

$$\vec{\rho}' = \dot{h}\hat{n} + h\dot{\hat{n}} + \dot{\epsilon}(\vec{r}_r \cos \theta + \vec{r}_i \sin \theta) + \epsilon(\vec{v}_r \cos \theta - \vec{r}_r \sin \theta \dot{\theta} + \vec{v}_i \sin \theta + \vec{r}_i \cos \theta \dot{\theta}) \quad (46)$$

The velocity is expressed as a function of the non-singular quantities as

$$\vec{\rho}' = [\dot{R}]\vec{z} + [R]\dot{\vec{z}} \quad (47)$$

where the time derivative of $[R]$ is

$$[\dot{R}] = \left[\dot{\hat{n}} \quad \vec{v}_r \quad \vec{v}_i \right] \quad (48)$$

To compute the rate of change of the elements, $\dot{\vec{z}}$, the time derivative of \vec{z} is first computed using the Cartesian relative position and velocity as

$$\dot{\vec{z}} = [R]^{-1} \left(\vec{\rho}' - [\dot{R}]\vec{z} \right) \quad (49)$$

The rate of change of ϵ is computed as

$$\dot{\epsilon} = \frac{\alpha \dot{\alpha} + \beta \dot{\beta}}{\epsilon} \quad (50)$$

Finally, the rate of change of θ is computed as

$$\dot{\theta} = \frac{\alpha\dot{\beta} - \beta\dot{\alpha}}{\epsilon^2} \quad (51)$$

The singularity at $\epsilon = 0$ appears in the mapping from elements to velocity, corresponding to the chaser lying on the \hat{n} axis. However, alternative formulations can be introduced as needed to avoid the singularity, including using the non-singular quantities \vec{z} and $\dot{\vec{z}}$. As an element set, the non-singular quantities provide linear mappings between Cartesian states, but do not provide the same geometric insight into relative motion as the geometric relative orbital elements \vec{e} and $\dot{\vec{e}}$.

Description of Natural Motion using Relative Elements

To demonstrate an implementation of the relative orbital element set to rapidly establish a relative trajectory based on quasi-periodic relative motion, an example of a spacecraft formation in the Earth-Moon system is explored. Using the CR3BP as the dynamical model for the Earth-Moon system, the target spacecraft is placed in an EM L_2 southern NRHO with a period of approximately 6.1 days in the EM rotating frame. The orbit of the target spacecraft is visualized in the rotating frame in Figure 5 along with the location of the Moon and EM L_2 .

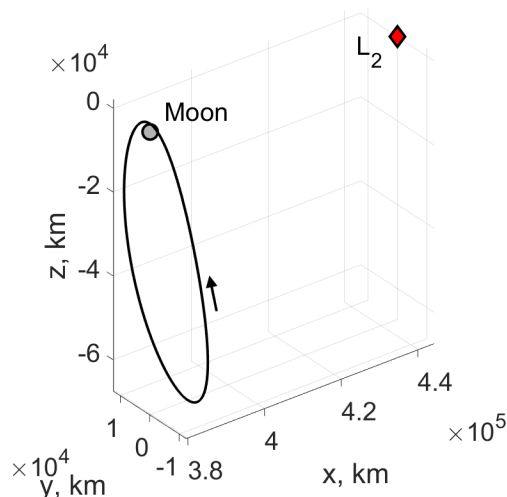


Figure 5. The target spacecraft periodic orbit: an Earth-Moon L_2 southern NRHO with a period of approximately 6.1 days.

The state of the chaser spacecraft is defined using the relative orbital element set, initialized at the apoapsis of the target spacecraft's orbit. To establish relative motion on first-order quasi-periodic relative motion, ϵ and θ are free parameters, while h , \dot{h} , $\dot{\epsilon}$, and $\dot{\theta}$ must equal 0. For first-order quasi-periodic motion to suitably approximate nonlinear quasi-periodic motion, ϵ must be small relative to the distance of the target from the two primary bodies. A chaser element set is selected as

$$\vec{e} = \begin{bmatrix} 0 \text{ km} \\ 10 \text{ km} \\ 0 \text{ rad} \end{bmatrix} \quad \dot{\vec{e}} = \begin{bmatrix} 0 \text{ km/s} \\ 0 \text{ km/s} \\ 0 \text{ rad/s} \end{bmatrix}$$

The selected initial element set is geometrically interpreted as the chaser spacecraft lying on the center plane. Since the elements are defined at apoapsis, the eigenvector is normalized to align with

the principal axes of the quasi-periodic relative ellipse. An angle of $\theta = 0$ rad indicates that the chaser spacecraft position vector is aligned with the semi-major axis of the quasi-periodic ellipse, and the sizing $\epsilon = 10$ km indicates the initial separation of the chaser from the target is 10 km. The relative trajectory is propagated for two revolutions of the target spacecraft's orbit using the nonlinear LVLH equations of relative motion from Eq. 15. The relative trajectory is visualized in the LVLH frame centered at the target spacecraft in Figure 6, where the target spacecraft is depicted with a red marker. The relative state described using Cartesian states over time is plotted in Figure 7. The relative orbital element set over time for the same trajectory is plotted in Figure 8. While the relative Cartesian states are time varying, the relative orbital element set maintains more consistent values while describing a relative trajectory established on first-order quasi-periodic motion across the entire period of the NRHO. The element ϵ and θ remain near-constant to the initial chosen values of 10 km and 0 rad respectively. For all elements and element rates, a distinct peak is observed as the formation passes periapsis of the NRHO, an area of high sensitivity. However, after each periapsis, the trend of the elements and rates is to return to near initial values.

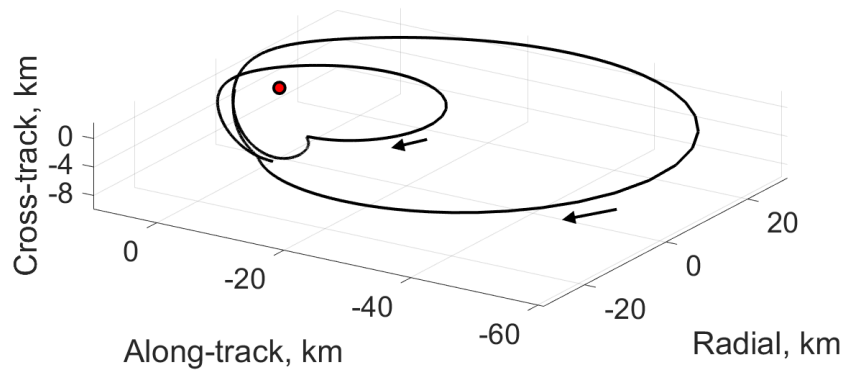


Figure 6. Trajectory of the chaser relative to the target spacecraft in the LVLH frame for two revolution of the NRHO.

TRANSFER DESIGN USING RELATIVE ORBITAL ELEMENTS

A two-point boundary variable problem can be solved via a single-shooting numerical corrections scheme. The use of relative orbital elements for relative transfer design has several benefits over Cartesian states including geometric insight into a state defined in elements, and increased consistency over the entire periodic orbit for near quasi-periodic motion. Two examples are explored to demonstrate the versatility of applying relative elements to design two-impulse formation reconfiguration maneuvers around different periodic orbits.

Example 1: Formation Reconfiguration using Impulsive Control

The first demonstrative example of the relative element set for transfer design is the reconfiguration of a formation of two spacecraft using impulsive maneuvers around a EM L_2 halo orbit. The halo orbit, illustrated in the rotating frame in Figure 9, possesses a period in the EM rotating frame of approximately 14.4 days. This type of transfer is inspired by formation reconfiguration between bounded relative motion in the two-body problem.^{12,24} For formation configuration around a three-body periodic orbit, the target spacecraft is assumed to travel along the periodic orbit. The desired chaser trajectory is a transfer between two relative ellipses defined by first-order quasi-periodic tori for a specified time-of-flight. Using the relative element set, the initial and final formation is defined

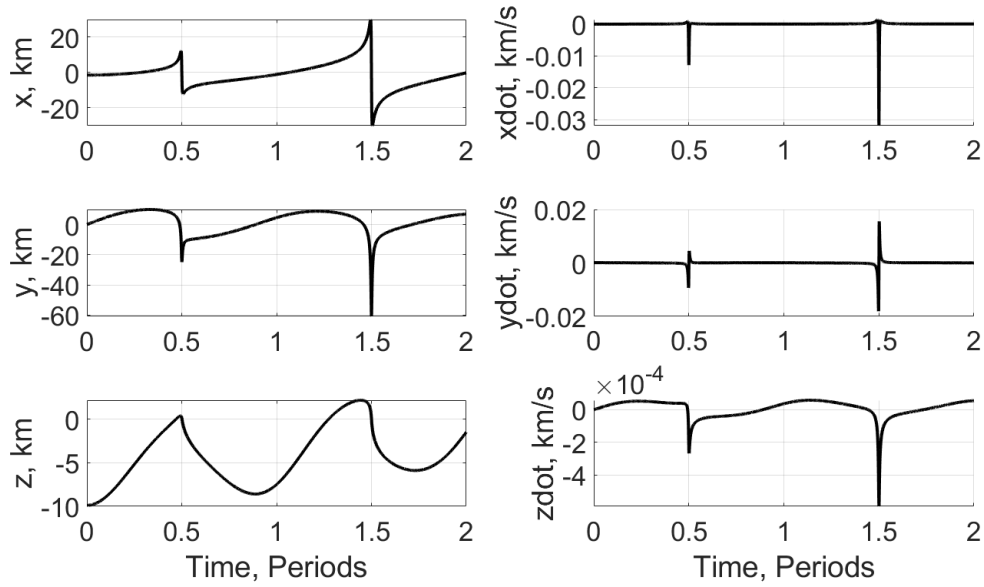


Figure 7. Cartesian relative states for the chaser spacecraft over two revolutions of the target spacecraft NRHO as visualized in Figure 6.

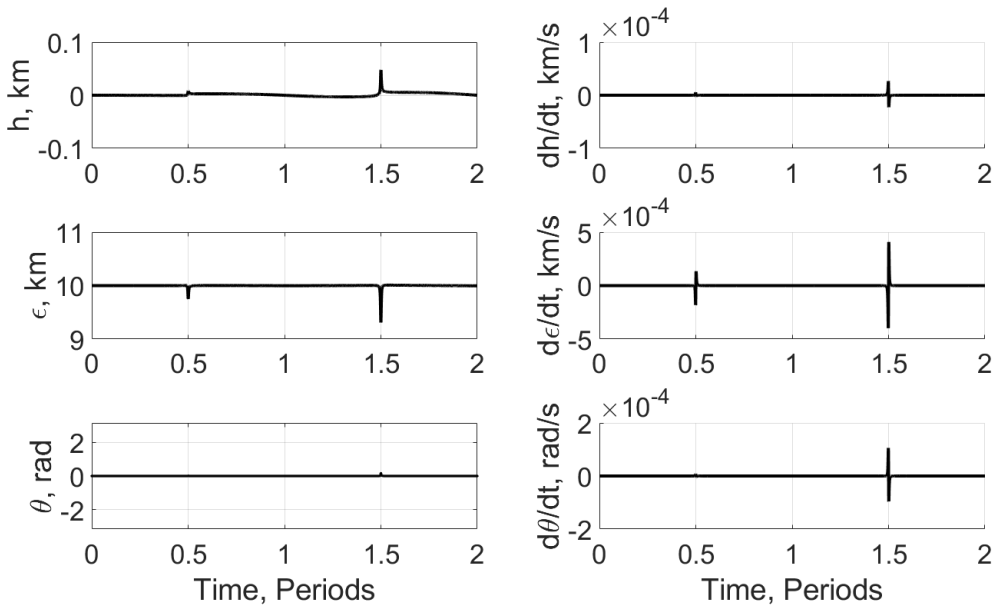


Figure 8. Relative orbital elements for the chaser trajectory over two revolutions of the target spacecraft NRHO visualized in Figure 6.

straightforwardly by selecting two values of ϵ and defining h , \dot{h} , $\dot{\epsilon}$, and $\dot{\theta}$ at the initial and final state equal to 0 to force first-order quasi-periodic relative motion.

A single-shooting algorithm is implemented by defining the free variable vector and constraint vector as a function of relative orbital elements. The value of the out-of-plane element at the final time h_f is constrained to equal zero, indicating the final state is on the center-plane. The final value of ϵ_f is constrained to equal the desired final value $\epsilon_{f,d}$. Lastly, rather than defining an arbitrary

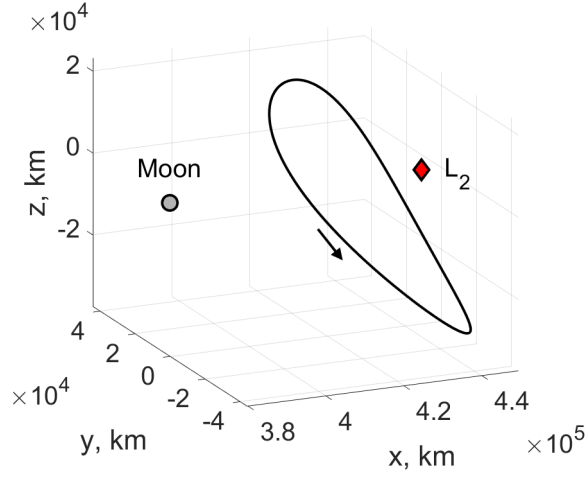


Figure 9. The target spacecraft periodic orbit: an Earth-Moon L_2 southern halo with a period of approximately 14.4 days.

constraint on the final angle element θ_f , the rate of change of ϵ at the final time, $\dot{\epsilon}_f$, is constrained to equal zero to ensure the geometry of the transfer approach to the final state is tangent to the final quasi-periodic ellipse. The complete constraint vector, defined before the second impulsive maneuver is applied, is written as

$$\vec{F} = \begin{bmatrix} h_f \\ \epsilon_f - \epsilon_{f,d} \\ \dot{\epsilon}_f \end{bmatrix} \quad (52)$$

such that the single-shooting algorithm converges when $|\vec{F}|$ is less than a specified tolerance. The free variable vector, \vec{V} , is defined as the initial rate of change of the relative orbital elements along the transfer as

$$\vec{V} = \begin{bmatrix} \dot{h}_0 \\ \dot{\epsilon}_0 \\ \dot{\theta}_0 \end{bmatrix} \quad (53)$$

The free variable vector that satisfies the constraint vector to within a specified tolerance is solved by iteratively applying Newton's method to update the constraints vector using the update equation

$$\vec{V}_{i+1} = \vec{V}_i - [DF]_i^{-1} \vec{F}_i \quad (54)$$

where $[DF]$ is the Jacobian of the constraint vector with respect to the free variable vector, computed using first-order forward finite difference at each iteration. For each iteration, the initial state of the transfer defined using relative elements, is converted to a relative Cartesian state vector and propagated using the equations of motion defined by Eq. 15. At the end of the transfer, the final Cartesian states are converted to elements to compute the constraint vector. The update process is continued until the Euclidean norm of the constraint vector is sufficiently small, to within a specified tolerance; a tolerance of 1×10^{-11} is used in this work.

An example scenario is explored to demonstrate the shooting algorithm in conjunction with the relative element set. The initial state of the chaser spacecraft is defined relative to the target spacecraft at the target spacecraft's apoapsis using relative elements $h_0 = 0$, $\epsilon_0 = 20$ km, and $\theta_0 = 0$. The desired final value of ϵ is $\epsilon_{f,d} = 5$ km. The maneuver time-of-flight is fixed at $t_{int} = 0.1 T$,

or approximately 1.4 days. The convergence criteria of Newton's method requires an initial guess that is sufficiently close to a solution. The initial guess of the free variable vector is developed using insight from the relative orbital elements. Since the initial and desired final states are defined such that $\dot{h} = 0$ and θ is unconstrained, the initial guesses for \dot{h} and $\dot{\theta}$ are selected as 0. The initial guess for $\dot{\epsilon}_0$ is selected as a first-order difference between the initial and final desired value of ϵ using the maneuver time of flight, t_{int} , written as

$$\dot{\epsilon}_0 \approx \frac{\epsilon_{f,d} - \epsilon_0}{t_{int}} \quad (55)$$

Using this initial guess, 5 iterations of the update equation are required for the Euclidean norm of the constraint vector to converge to below the specified tolerance. The required Δv is 0.140 m/s for the first impulsive maneuver and 0.149 m/s for the second maneuver, for a total transfer Δv of 0.289 m/s. The resulting reconfiguration trajectory is illustrated in the LVLH frame in Figure 10, where the target spacecraft is depicted using a red circle. The initial chaser state is denoted with a black triangle and the final chaser state is denoted with a black cross. The initial relative ellipse defined by ϵ_0 at the initial time t_0 and ϵ_f and the final time t_f are illustrated by dotted black lines. The constraint formulation developed as a function of relative orbital elements provides geometric insight into the impulsive transfer which may be more challenging to represent as a function of Cartesian states. Furthermore, the low number of iterations required to converge on a solution highlights how the relative element set provides an intuitive initial guess for a transfer of this nature.

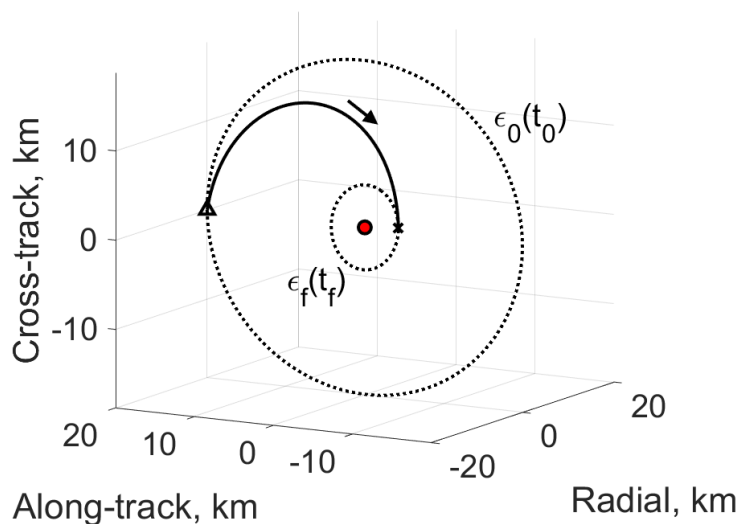


Figure 10. Visualization of the relative trajectory in the LVLH frame for a transfer between first-order quasi-periodic relative motion of different size.

Example 2: Formation Deployment using Impulsive Control

The elements ϵ and θ may be used to establish a chaser state in a first-order bounded trajectory relative to the target at any point along the reference periodic orbit. Additionally, the relative elements may be applied to different reference periodic orbits with oscillatory modes. The second demonstration of trajectory design with the relative elements is an example of deploying a spacecraft from an EM DRO to a first-order quasi-periodic tori in its vicinity. The target spacecraft is defined on an

EM DRO reference orbit with a period in the rotating frame of approximately 4.8 days, illustrated in Figure 11 in the EM rotating frame. The initial state of the target spacecraft along the DRO lies along the \hat{x} axis of EM rotating frame between L_1 and the Moon, with a positive \dot{y} component.

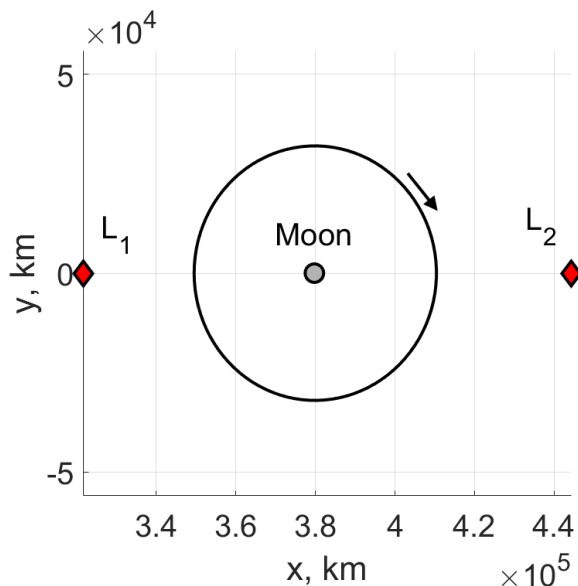


Figure 11. Earth-Moon DRO of the target spacecraft with a period of 4.8 days.

The second example explores the deployment of a chaser spacecraft from the target spacecraft to establish a formation. The initial state of the chaser is coincident with the target spacecraft. The same constraint formulation from Eq. 52 is applied. However, since the description of the relative elements is singular at the origin, the time rate-of-change of the non-singular quantities, $\dot{\vec{z}}$, is used as the free variables in the single-shooting scheme, written as

$$\vec{V} = \begin{bmatrix} \dot{h}_0 \\ \dot{\alpha}_0 \\ \dot{\beta}_0 \end{bmatrix} \quad (56)$$

Similar to the previous example, the initial guess for the free variable vector is generated using the average rate of change between the desired ϵ , $\epsilon_{f,d}$ and the origin. The initial guess for $\dot{\alpha}_0$ is

$$\dot{\alpha}_0 \approx \frac{\epsilon_{f,d}}{t_{int}} \quad (57)$$

and the initial guesses for \dot{h} and $\dot{\beta}$ are set to 0.

With the free variable and constraint formulation defined, example transfer parameters are defined for the second example. The final desired ϵ is equal to 30 km for a time-of-flight equal to $0.5 T$, or approximately 2.4 days. Using the initial guess formulation, 5 iterations are required to converge to a solution that satisfies the constraint stopping criteria of $|\vec{F}| < 1 \times 10^{-11}$. The required Δv is 0.126 m/s for the first impulsive maneuver and 0.064 m/s for the second maneuver, for a total transfer Δv of 0.190 m/s. The deployment trajectory is plotted in the LVLH frame in Figure 12 with the relative ellipse defined by ϵ_f at the final time. This transfer shares geometric similarities

with the previous transfer explored around the EM halo orbit. This is an intuitive result, as the same constraint description using relative elements at the final time was applied. Furthermore, the singularity that exists for the relative element set at $\epsilon = 0$ is avoided by applying the alternative non-singular elements to describe the initial transfer velocity. Similar to the previous example, a low number of iterations is required to converge on a solution. This highlights how the non-singular element set provides a suitable initial guess for a transfer from the origin of the LVLH frame.

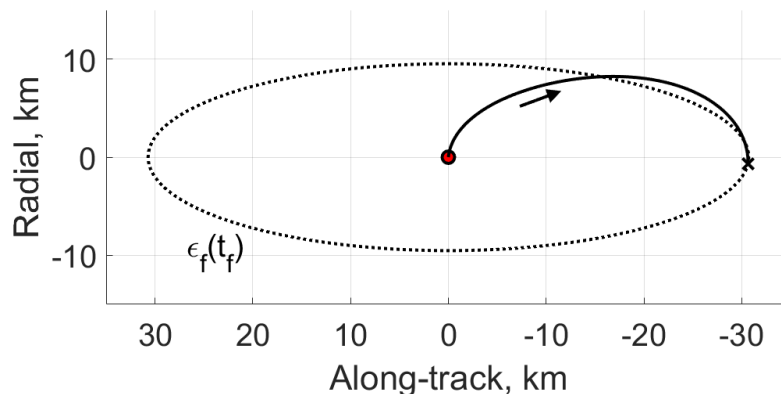


Figure 12. Deployment transfer from an EM DRO to first-order quasi-periodic relative motion.

CONCLUSIONS

Equations of relative motion in a local-vertical, local-horizontal frame are presented to describe the relative dynamics of a chaser spacecraft relative to a target spacecraft in a three-body environment. A relative orbital element set based on first-order quasi-periodic motion is introduced to describe motion relative to periodic orbits in the CR3BP with oscillatory modes and provide a more consistent state description of spacecraft states over time near quasi-periodic motion. Two demonstrations are explored that leveraged the geometric insight of the relative elements to establish and reconfigure spacecraft formations using impulsive maneuvers near an Earth-Moon halo orbit and an Earth-Moon distant retrograde orbit. While a singularity exists within the mappings between the relative orbital element and relative Cartesian states, an alternative non-singular element set is also presented, and an example of a transfer design avoiding the singularity is analyzed. The relative orbit element set may be used to more consistently describe spacecraft formations, develop constraint formulations for single-shooting targeting schemes, and develop initial guesses for impulsive transfers for different fixed points along a periodic orbit. Further, as the relative element set is well-suited for application to different reference periodic orbits, this element representation has broad applications to formation flying missions in three-body environments.

ACKNOWLEDGMENTS

Presentation at this conference was supported by a Beverly Sears Graduate Student Grant from the University of Colorado Boulder.

REFERENCES

- [1] W. H. Clohessy and R. S. Wiltshire, “Terminal Guidance System for Satellite Rendezvous,” *Journal of the Aerospace Sciences*, Vol. 27, No. 9, 1960, pp. 653–658, 10.2514/8.8704.

- [2] P. Sengupta and S. R. Vadali, "Relative Motion and the Geometry of Formations in Keplerian Elliptic Orbits with Arbitrary Eccentricity," *Journal of Guidance, Control, and Dynamics*, Vol. 30, No. 4, 2007, pp. 953–964, 10.2514/1.25941.
- [3] J. Sullivan, S. Grimberg, and S. D'Amico, "Comprehensive Survey and Assessment of Spacecraft Relative Motion Dynamics Models," *Journal of Guidance, Control, and Dynamics*, Vol. 40, No. 8, 2017, pp. 1837–1859, 10.2514/1.G002309.
- [4] G. Franzini and M. Innocenti, "Relative Motion Dynamics in the Restricted Three-Body Problem," *Journal of Spacecraft and Rockets*, Vol. 56, No. 5, 2019, pp. 1322–1337, 10.2514/1.A34390.
- [5] G. Franzini and M. Innocenti, "Relative Motion Dynamics with Arbitrary Perturbations in the Local-Vertical Local-Horizon Reference Frame," *Journal of the Astronautical Sciences*, 03 2020, pp. 98–112, 10.1007/s40295-019-00185-0.
- [6] T. A. Lovell and S. Tragesser, *Guidance for Relative Motion of Low Earth Orbit Spacecraft Based on Relative Orbit Elements*. 2004, 10.2514/6.2004-4988.
- [7] L. M. Healy and C. G. Henshaw, "Trajectory Guidance Using Periodic Relative Orbital Motion," *Journal of Guidance, Control, and Dynamics*, Vol. 38, No. 9, 2015, pp. 1714–1724, 10.2514/1.G000945.
- [8] T. Bennett and H. Schaub, "Continuous-Time Modeling and Control Using Nonsingular Linearized Relative-Orbit Elements," *Journal of Guidance, Control, and Dynamics*, Vol. 39, No. 12, 2016, pp. 2605–2614, 10.2514/1.G000366.
- [9] J. L. Goodman, "History of Space Shuttle Rendezvous and Proximity Operations," *Journal of Spacecraft and Rockets*, Vol. 43, No. 5, 2006, pp. 944–959, 10.2514/1.19653.
- [10] D. S. Koons and C. Schreiber, *Risk Mitigation Approach to Commercial Resupply to the International Space Station*. 2010.
- [11] P. V. Anderson and H. Schaub, "N-Impulse Formation Flying Feedback Control Using Nonsingular Element Description," *Journal of Guidance, Control, and Dynamics*, Vol. 37, No. 2, 2014, pp. 540–548, 10.2514/1.60766.
- [12] C. W. T. Roscoe, J. J. Westphal, J. D. Griesbach, and H. Schaub, "Formation Establishment and Reconfiguration Using Differential Elements in J2-Perturbed Orbits," *Journal of Guidance, Control, and Dynamics*, Vol. 38, No. 9, 2015, pp. 1725–1740, 10.2514/1.G000999.
- [13] B. T. Barden and K. C. Howell, "Fundamental Motions Near Collinear Libration Points and Their Transitions," *Journal of the Astronautical Sciences*, Vol. 46, No. 4, 1998, pp. 361–378.
- [14] G. Gómez and J. Mondelo, "The Dynamics Around the Collinear Equilibrium Points of the RTBP," *Physica D: Nonlinear Phenomena*, Vol. 157, No. 4, 2001, pp. 283 – 321, 10.1016/S0167-2789(01)00312-8.
- [15] B. G. Marchand and K. C. Howell, "Control Strategies for Formation Flight in the Vicinity of the Libration Points," *Journal of Guidance, Control, and Dynamics*, Vol. 28, No. 6, 2005, pp. 1210–1219, 10.2514/1.11016.
- [16] M. Bando and A. Ichikawa, "Formation Flying Along Halo Orbit of Circular-Restricted Three-Body Problem," *Journal of Guidance, Control, and Dynamics*, Vol. 38, No. 1, 2015, pp. 123–129, 10.2514/1.G000463.
- [17] D. J. Scheeres, F.-Y. Hsiao, and N. X. Vinh, "Stabilizing Motion Relative to an Unstable Orbit: Applications to Spacecraft Formation Flight," *Journal of Guidance, Control, and Dynamics*, Vol. 26, No. 1, 2003, pp. 62–73, 10.2514/2.5015.
- [18] N. Baresi, D. J. Scheeres, and H. Schaub, "Bounded Relative Orbits About Asteroids for Formation Flying and Applications," *Acta Astronautica*, Vol. 123, 2016, pp. 364–375, 10.1016.
- [19] N. Bosanac, *Leveraging Natural Dynamical Structures to Explore Multi-Body Systems*. PhD thesis, Purdue University, West Lafayette, IN, 2016.
- [20] Z. P. Olikara and D. J. Scheeres, "Numerical Methods for Computing Quasi-Periodic Orbits and their Stability in the Restricted Three-Body Problem," *Advances in the Astronautical Sciences*, 2012, pp. 911–930.
- [21] W. McClain and D. Vallado, *Fundamentals of Astrodynamics and Applications*. Space Technology Library, Springer Netherlands, 2001.
- [22] W. S. Koon, M. W. Lo, J. E. Marsden, and S. D. Ross, *Dynamical Systems, the Three-Body Problem and Space Mission Design*. 2006. Marsden Books.
- [23] H. Schaub and J. Junkins, *Analytical Mechanics of Space Systems*. AIAA Education Series, American Institute of Aeronautics and Astronautics, Incorporated, 2014.
- [24] S. S. Vaddi, K. T. Alfriend, S. Vadali, and P. Sengupta, "Formation Establishment and Reconfiguration using Impulsive Control," *Journal of Guidance, Control, and Dynamics*, Vol. 28, No. 2, 2005, pp. 262–268, 10.2514/1.6687.